Efficient and Reliable Wireless Communications via Multi-Connectivity using Rateless Codes in Single- and Multi-User Scenarios

Philipp Schulz, *Member, IEEE,* Andreas Traßl, André Noll-Barreto, *Member, IEEE,* and Gerhard Fettweis, *Fellow, IEEE*

Abstract—Due to the great flexibility and innate simplicity of wireless networks, many applications are now realized with wireless connectivity at their core. Countless novel applications are enabled this way and legacy applications are transferred to mobile networks to reap the same benefits. As the networks evolve, applications are becoming ever more demanding, particularly with respect to high reliability and low latency. A common way to achieve high reliability in wireless communications is adding redundant communication channels by means of multi-connectivity. This comes at the cost of additional radio resources that could have been used by other connections. However, multiple links are not always required to achieve the desired reliability. Thus, we propose to combine multi-connectivity with rateless coding as a strategy for efficient resource usage in reliable wireless communications. The proposed schemes consider an erasure channel, and can therefore be implemented on the application layer, making them suitable for use with different physical layer wireless technologies simultaneously. We start out with a single-user analysis and then extend our discussion to multi-user scenarios. Our approach is compared against standardized packet duplication with our analytical framework and by means of simulation. The results with rateless coding show significant gains with respect to the required resources and feedback transmissions.

Index Terms—Reliability, Efficiency, Multi-Connectivity.

I. INTRODUCTION

ALONG with the development of fifth generation (5G) mobile networks, entirely new applications are envisioned, including the class of ultra-reliable low latency communications (URLLC) [1]. URLLC comprises applications, e. g., in control scenarios, with extremely high requirements on latency and reliability that have only been feasible with cable-based implementations in the past, the main obstacle being the random nature of the wireless medium. However, great flexibility and simple setup (among others) make wireless solutions very appealing. Furthermore, many novel applications are not realizable with cables at all, e. g., teleoperated driving [2].

Nevertheless, reliability and latency do not always go hand-in-hand, and so [3] differentiates between low latency communications (LLC), ultra-reliable communications (URC), and the most challenging URLLC, combining both. This perspective is supported by earlier work [4], which classifies "long-" and "short-term URC", where the latter refers to URLLC as introduced in [3]. In this paper, we focus on URC. Exemplary applications can be found in intelligent transport systems (ITS), which allow up to a few tens of milliseconds of latency [5], [6], or in other fields such as process automation [7], e-health, or banking.

To achieve extremely high reliability, some redundancy has to be added, for instance by provisioning parallel redundant transmission channels. However, redundancy can be wasteful, when there are no channel outages, leading to a reduction in overall system capacity. Hence, the challenge arises to design systems not only to be reliable, but also efficient.

This challenge was already identified by the research community (e. g., [8]–[12]), and the task is even more difficult when other services, especially resource-hungry enhanced mobile broadband (eMBB) services, are present at the same time [8], [9]. In [8], a joint preference metric is introduced to offer efficient resource allocation when eMBB and URLLC coexist. [9] provides an overview of key technology components to enable URLLC. Another set of URLLC enablers on the physical layer (PHY) is introduced in [10], including waveform multiplexing, multiple-access schemes, channel code design, synchronization, and full-duplex transmission for spectrally efficient URLLC. In [11] the major impact of feedback on the efficiency is highlighted, and an optimum harmonization of feedback-based and feedback-less transmissions through multi-armed bandit-based reinforcement learning is proposed to improve efficiency. In order to optimize resource allocation in URLLC for wireless control systems, the authors of [12] follow a communications-control codesign (CoCoCo) approach, where control requirements are mapped to communication requirements. CoCoCo enables resource-efficient adaptive communication systems that respect the requirements of control applications. For instance, [13] proposes a state-aware resource allocation scheme, that increases the number of parallel links for agents that recently suffered from packet losses, which is shown to be extremely efficient for control applications that can tolerate packet loss, as long as the number of consecutive losses is limited.

In this paper, we consider multi-connectivity (MC), which

is widely seen as a promising technique to ensure high reliability [2], [14], and apply rateless codes (RCs) to retain efficiency. Both concepts are discussed in more detail in the subsequent Sections I-A and I-B.

A. Multi-Connectivity

To realize URC transmitting redundant copies of data is a promising strategy. In wireless communications, this can be realized through time, space, or frequency diversity. Distributing information over time, e. g., through automatic repeat request (ARQ) or the more efficient hybrid ARQ (HARQ), however induces latency by design, and does not work in static scenarios, as it depends on channel variations over time. In contrast, spatial or frequency resources can be utilized in parallel by establishing multiple links, which is summarized as MC. The diversity concepts can be further classified as follows [15]. Spatial diversity can be realized through multiple antennas at transmitters and/or receivers to combat small-scale fading, which is referred to as micro-diversity. It can also be exploited by antennas that are separated by far more than the wave length, e. g., by using multiple base stations (BSs) or access points (APs), which is denoted as macro-diversity and has the ability to counteract large-scale fading effects. On the other hand, frequency diversity is divided into intra-frequency and inter-frequency diversity, depending on whether the same or different frequency bands are being used. In addition, the authors of [16] introduced the term interface diversity, proposing that multiple technologies, such as 5G, wireless local area network (WLAN), or Bluetooth, may be utilized simultaneously. However, as tight coordination is not possible on multiple interfaces, technology-agnostic approaches are required.

MC can be used not only to enhance reliability by transmitting redundant data, but also to increase the achievable data rate by sending independent data. The authors of [17] developed an analytical framework to study a trade-off between these contrary goals.

MC is already considered in the Third Generation Partnership Project (3GPP) standardization, by introducing packet duplication on multiple links [18]. Packet duplication constitutes a relatively simple approach, as it does not require tight cooperation of the transmitters. However, simply duplicating packets is a "wasteful" scheme, as there is no benefit when more than one of the transmissions succeeds. A more sophisticated approach is given by coordinated multipoint (CoMP) [19], [20], which also includes the special case of maximum ratio combining (MRC), where devices are connected to several BSs simultaneously and can benefit from dynamic inter-cell scheduling coordination or joint transmission/reception from/at multiple transceivers. However, CoMP requires tight cooperation between the participating sites, occupies multiple resources through joint transmission/reception and usually increases complexity.

Another way to overcome the inefficiencies of duplication can be pursued through coding. For instance, the authors of [21] apply a K-out-of-$\tilde{K}$ erasure code for a reliable multi-path fronthaul with efficient resource usage. While this approach offers an efficient scheme, it is not very flexible, as a code rate has to be fixed in advance and feedback knowledge is required, if the transmission still fails. To overcome this drawback, we study the application of RCs for reliable wireless communications. However, we consider the air interface rather than the fronthaul.

B. Rateless Codes in Wireless Communications

RCs [22] are erasure codes that automatically adapt their rate to the current conditions. Thus, in contrast to other codes, there is no code rate to be configured a priori. Instead, the actual code rate depends on the experienced loss. An arbitrary amount of encoded packets can be generated until decoding is successful. A common metaphor is the collection of droplets of a fountain with a bucket. Hence, they are also called *fountain codes*. Popular examples of RCs are random linear fountain codes, such as Luby transform (LT) codes [23], which focus on efficient decoding for large amounts of data, and raptor codes [24], [25]), which improve the decoding properties of LT codes by adding an outer erasure code. The technical aspects of RCs will be briefly recapped in Section II-C2.

As they are primarily designed for high packet numbers, RCs are already popular where large amounts of data are involved, e. g., in the context of (satellite) video broadcasting [26], (cloud) data storage [27], or peer-to-peer networks [28]. Accordingly, raptor codes are already standardized for 3GPP multimedia broadcast and multicast service (MBMS) [29] and, thus, constitute a part of the application layer.

RCs found various applications in wireless communications. For instance, [30] and references therein apply RCs on the PHY. Thereby, the authors consider large numbers of message symbols greater or equal than 2000. The authors of [31], [32] propose an analogue fountain code (AFC) for a multiple access scheme, where encoded packets from different users sum up to a new AFC. Thereby, the media access control (MAC) layer is being addressed. However, the approach requires tight synchronization between the users and also considers large numbers of packets. More recently, [33], [34] proposed RCs for multi-user downlink (DL) and uplink (UL), respectively, for cloud radio access network (C-RAN). Nonetheless, the authors coded user data individually and also considered long message lengths. In contrast, we consider short messages and propose a joint encoding in a multiplexing scheme for multiple users. In [35], raptor codes have been used to design a robust and efficient relaying framework, but therein, only a very long information block length has been considered. RCs were also applied to multiple-input multiple-output (MIMO), e. g., in [36]–[38]. In contrast to our approach, these works operate on lower levels and consider additive white Gaussian noise (AWGN) channels.

To the best of our knowledge RCs have not received much attention in the area of URC so far, where short packets sizes are common. One example of RCs in URC is provided in [39]. The authors propose raptor codes in order to increase the reliability of millimeter wave communications. The authors study the key performance indicators (KPIs) packet loss and throughput, based on a millimeter wave simulator, but do not provide any mathematical modeling.

We proposed a similar approach in [40], where we used RCs in the context of URC. In contrast to [39], we focus on the efficiency, with respect to radio resources as well as feedback messages, where we do not only rely on our simulations, but also developed an analytical framework.

It should also be noted that RCs are related to random linear network codes [41]. However, they differ conceptually, since RCs are primarily erasure codes, whereas network codes are conceptualized as a combining scheme to outperform traditional routing in a network.

C. Contribution and Organization of this Article

Our key contributions are the following:

1) We revise our previous work [40], which contains a flaw regarding outer codes, and show that our proposed schemes are still beneficial with respect to radio resource and feedback efficiency without adding an outer code.
2) We extend our single-user investigation in [40] by considering multiple users.
3) By utilizing a WLAN simulator, we consolidate our results in a more realistic scenario.
4) We propose a novel multi-user multiplexing scheme based on RC. This approach requires less packets of each user for coding as an important step towards low-latency applications.
5) Our approaches consider rather small numbers of packets to be transmitted, in contrast to existing works on RC that mainly consider large packet numbers.
6) For all considered schemes, we provide an analytical framework for uncorrelated channels.

The remainder of this article is organized as follows. Section II provides the general system model. In Sections III and IV we introduce the investigated MC schemes along with the mathematical modeling of the random distributions of the KPIs of interest. The investigated simulation scenarios are described in Section V, before they are used to validate the models and to evaluate the MC schemes in Section VI. Finally, Section VII concludes and provides an outlook.

II. SYSTEM MODEL

In this section, we briefly summarize the system model used in this paper. It will be described in more detail in Sections III and IV for the single- and the multi-user case, respectively.

A. Notation and Definitions

The complement of a probability p is denoted as $\bar{p} := 1 - p$. The indicator function $\chi_A(x)$ of a set A is one, if $x \in A$ and zero otherwise. The operator $[a_r]_{r=1}^K$ defines a vector via the components a_r. Finally, $\lceil \cdot \rceil$ denotes the ceiling operator.

B. Scenario

All devices considered in this paper are connected via L links to a wireless AP and have to transmit a payload of K packets. For these links, we state the following assumption:

Assumption 1 (Independent links): All wireless links are independent from each other.

This assumption can be satisfied, e. g., by using carriers that are separated by at least the coherence bandwidth of the channel or by spatially distributed antennas. We also assume Rayleigh fading on all links. However, the approach is not restricted to Rayleigh fading and could be easily extended to other fading models, such as Rician or Nakagami-m fading.

We aim for a technology-agnostic approach by operating on the application-layer. Thus, APs can use cellular, WLAN, or any other wireless technology. This approach offers great flexibility and does not need synchronization of multiple transmitters (or receivers) except for the feedback handling. Furthermore, for some applications, especially in the context of CoCoCo [13], it might be beneficial to let the application decide on additional redundant packet transmissions, depending on the importance of the lost information. For instance, in automative applications, frequent updates are required particularly at high velocities, whereas there is no need for updates, when the vehicle stands still. With respect to the application-layer perspective, we assume the following:

Assumption 2 (Binary erasure channel (BEC)): Received packets are either correctly received or completely lost, such that we deal with a BEC.

Hence, we assume that possible packet errors are handled by lower layers, if possible. If they cannot be corrected, a packet is considered as lost, i. e., not received, on the application layer.

C. Multi-Connectivity Schemes

We study and compare different MC schemes, which are explained in this Section.

1) Selection Combining: Selection combining (SC) has already been standardized by 3GPP as packet duplication or dual connectivity (DC) [18]. Hence, it is taken as the baseline to benchmark our approach. Within this scheme, packets are duplicated and the resulting copies are sent over all L links to the receiver. The transmission is successful, if at least one of these copies is successfully received. This scheme is relatively easy to implement and, in contrast to CoMP [19], strict synchronization of multiple transmitters (or receivers) is not required, as only the feedback has to be coordinated. Based on Assumption 1 and with $p_{\text{tx},l}$ being the success probability of the l-th link ($l \in \{1, ..., L\}$), the success probability of a packet duplicated on independent links can be expressed as follows:

$$p_{\text{tx}} = 1 - \prod_{l=1}^{L} \bar{p}_{\text{tx},l}. \qquad (1)$$

For equally strong links with the same packet loss rate (PLR), (1) simplifies to $p_{\text{tx}} = 1 - \bar{p}_{\text{tx},l}^L$.

2) Rateless Coding: For the sake of convenience, we briefly recap the concept of RC here. However, the interested reader is referred to [22] for more details.

The idea of RCs is to allow the generation of arbitrarily many encoded packets. A receiver collects these packets until it can decode the data. As it is not possible to determine the required number of encoded packets a priori, RCs do not exhibit a fixed code rate and hence their name. Accordingly, no knowledge about the BEC and its PLR is required in advance

to setup an appropriate code rate. Furthermore, if packets are lost, no feedback about which specific packets have been lost is necessary, since additional new packets can be generated independently for further transmissions.

Usually, the required number of packets for decoding an RC is random as it depends on the specific packets that have been received successfully. A common class of RCs is given by the LT codes [23]. They can be configured in a way that around $1.05K$ encoded packets are sufficient to recover the original K packets [22] with high probability. We will elaborate more on the decoding failure probability in Section II-D. LT codes are designed to allow efficient decoding by keeping the generator matrix sparse, which is especially beneficial to encode large amounts of data. In this situation, the decoding performance can be significantly improved by adding an additional outer code with a fixed rate, because LT codes are very likely to be able to decode all but a few packets if the number $\tilde{M}$ of received encoded packets slightly exceeds the number of original packets K and the outer code then recovers the few missing packets. A popular example of such a combined code is given by Raptor codes [24], which combine a low-density parity-check (LDPC) code and an LT code as the outer and inner code, respectively. However, for a comparably small number of packets as considered in this work, random linear fountain codes exhibit better decoding probability than LT codes (cf. Section II-D) and the outer code approach is not beneficial. Therefore, the general term of RCs always refers to random linear fountain codes in the remainder of this paper.

As other linear codes, a random linear fountain code can be described by a generator matrix $\boldsymbol{G}$. In contrast to the generator of other codes, this matrix has the dimensions $K \times \infty$ for fountain codes that encode the original K packets, as illustrated in Fig. 1. However, in practice only a finite, but arbitrarily high number M of columns is created. For random codes, each element of $\boldsymbol{G}$ is picked randomly from $\{0, 1\}$ with equal probability, but excluding the all-zeros column. Each column defines an encoded packet by a bit-wise xor operation of all packets where the entry is one. By defining a matrix multiplication $\otimes$ as follows:

$$\boldsymbol{Y} = \boldsymbol{X} \otimes \boldsymbol{G} := \left[\bigoplus_{i=1,\ldots,K} g_{ij} \boldsymbol{x}_i \right]_{j \in \mathbb{N}}, \qquad (2)$$

the encoding of the packets collected in $\boldsymbol{X} = [\boldsymbol{x}_1, \ldots, \boldsymbol{x}_{\tilde{K}}]$ to the encoded packets $\boldsymbol{Y} = [\boldsymbol{y}_1, \boldsymbol{y}_2, \ldots]$ is formulated in matrix-vector notation. Herein, the operator $\oplus$ denotes the bit-wise xor operation. In this regard, we define the space $\mathcal{K} := \mathrm{GF}(2)^K$ equipped with the multiplication with scalars from $\mathrm{GF}(2) = \{0, 1\}$ and the bit-wise xor $\oplus$ acting as the vector addition.

Only an identifier (ID) for each encoded packet is needed as overhead by using the same pseudo-random number generator (PRNG) at each terminal. The ID provides all necessary information by acting as the PRNG seed to reconstruct the corresponding column of $\boldsymbol{G}$.
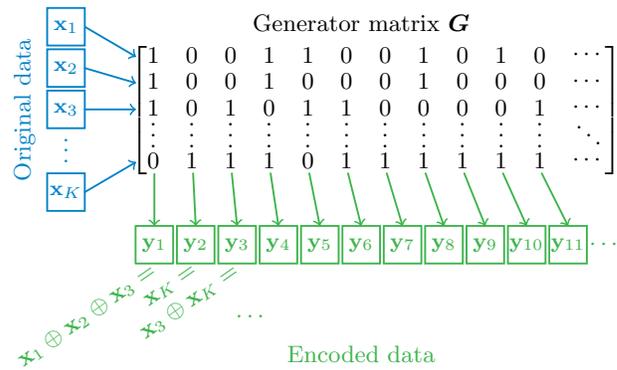

Fig. 1: Illustration of the coding scheme.

D. Decoding Failure Probability for RC

At a receiving terminal, only $\tilde{M}$ out of M sent packets are received due to potential packet loss. Let $\tilde{\boldsymbol{G}}^{(\tilde{M})}$ denote the corresponding $K \times \tilde{M}$ part of $\boldsymbol{G}$. Decoding is possible, if (2) can be solved for $\boldsymbol{X}$, if $\boldsymbol{G}$ is replaced by $\tilde{\boldsymbol{G}}^{(\tilde{M})}$, i. e., if $\tilde{\boldsymbol{G}}^{(\tilde{M})}$ has full rank in the xor arithmetic:[1]

$$\mathrm{rank}\, \tilde{\boldsymbol{G}}^{(\tilde{M})} = K. \qquad (3)$$

For the subsequent derivation of the decoding failure probability, the approach from [24, Appendix A] is applied to our scenario. The idea is to inductively add columns to the generator matrix and calculate the probability that this operation increases the rank. Therefore, let r be the rank of the generator matrix of the received packets, which is equivalent to the dimension of the subspace $\mathcal{G}^{(\tilde{M})}$ that is spanned by the columns of $\tilde{\boldsymbol{G}}^{(\tilde{M})}$:

$$r := \mathrm{rank}\, \tilde{\boldsymbol{G}}^{(\tilde{M})} = \dim\left(\mathrm{span}\, \tilde{\boldsymbol{G}}^{(\tilde{M})}\right) = \dim \mathcal{G}^{(\tilde{M})}. \qquad (4)$$

If we now randomly pick a new column $\boldsymbol{g}^{(\tilde{M})} \in \mathcal{K} \setminus \{\boldsymbol{0}\}$ and append it to $\tilde{\boldsymbol{G}}^{(\tilde{M})}$, such that

$$\tilde{\boldsymbol{G}}^{(\tilde{M}+1)} = \left[\tilde{\boldsymbol{G}}^{(\tilde{M})} \,\middle|\, \boldsymbol{g}^{(\tilde{M})} \right], \qquad (5)$$

this increases the rank by one if the new column $\boldsymbol{g}^{(\tilde{M})}$ is not in $\mathcal{G}^{(\tilde{M})}$. Otherwise, the rank does not change. Hence, the probability can be expressed through the cardinalities of $\mathcal{G}^{(\tilde{M})}$ and $\mathcal{K}$:

$$\mathbb{P}\left\{ \mathrm{rank}\, \tilde{\boldsymbol{G}}^{(\tilde{M}+1)} = r \right\} = \frac{|\mathcal{G}^{(\tilde{M})}| - 1}{|\mathcal{K}| - 1}$$
$$= \frac{2^r - 1}{2^K - 1} =: \bar{q}_r^{(\tilde{M}+1)}, \qquad (6a)$$

$$\mathbb{P}\left\{ \mathrm{rank}\, \tilde{\boldsymbol{G}}^{(\tilde{M}+1)} = r + 1 \right\} = 1 - \bar{q}_r^{(\tilde{M})} = q_r^{(\tilde{M}+1)}. \qquad (6b)$$

Now, the probability mass functions (PMFs) for the rank distribution of $\tilde{\boldsymbol{G}}^{(\tilde{M})}$, i. e.,

$$\boldsymbol{r}^{(\tilde{M})} = \left[r_r^{(\tilde{M})} \right]_{r=1}^{K} = \left[\mathbb{P}\left\{ \mathrm{rank}\, \tilde{\boldsymbol{G}}^{(\tilde{M})} = r \right\} \right]_{r=1}^{K} \qquad (7)$$

---

[1] Our previous work [40] contains the flaw that for a precoding K-out-of-$\tilde{K}$ outer code, which enlarges $\tilde{\boldsymbol{G}}^{(\tilde{M})}$ to the dimensions $\tilde{K} \times \tilde{M}$ for a $\tilde{K} > K$, it is possible to recover the original K packets, if $\mathrm{rank}\, \tilde{\boldsymbol{G}}^{(\tilde{M})} \geq K$. However, this condition is only necessary, but not sufficient. Accordingly, we remove this error in the paper at hand and present only corrected results.

are under consideration. It should be noted that the case $r = 0$ is excluded here, as $\tilde{\boldsymbol{G}}^{(\tilde{M})}$ does not contain any zero column. The PMFs $\boldsymbol{r}^{(\tilde{M})}$ of the rank distribution for $\tilde{\boldsymbol{G}}^{(\tilde{M})}$ can be determined iteratively by starting with the trivial rank distribution of $\tilde{\boldsymbol{G}}^{(1)}$, since $\tilde{\boldsymbol{G}}^{(1)}$ has always rank one:

$$\boldsymbol{r}^{(1)} = \begin{bmatrix} 1 & 0 & \dots & 0 \end{bmatrix}. \tag{8a}$$

Then, for each $\tilde{M} \geq 1$, a new random column $\boldsymbol{g}^{(\tilde{M})}$ is added and (6) is applied to obtain the rank distribution for $\tilde{\boldsymbol{G}}^{(\tilde{M}+1)}$:

$$\boldsymbol{r}_r^{(\tilde{M}+1)} = \begin{cases} \bar{q}_r^{(\tilde{M})} \boldsymbol{r}_r^{(\tilde{M})}, & r = 1, \\ \bar{q}_r^{(\tilde{M})} \boldsymbol{r}_r^{(\tilde{M})} + q_{r-1}^{(\tilde{M})} \boldsymbol{r}_{r-1}^{(\tilde{M})}, & r > 1. \end{cases} \tag{8b}$$

This iterative scheme can be evaluated with quadratic computational effort. For the best case $\tilde{M} = K$, a rank has to be added in each step and, thus, the iterative procedure simplifies to:

$$\boldsymbol{r}_K^{(K)} = \prod_{r=1}^{K} q_r^{(r)} = \prod_{r=1}^{K} \left(1 - \frac{2^{r-1} - 1}{2^{\tilde{K}} - 1}\right). \tag{9}$$

Finally, the decoding success probability of an RC code for $\tilde{M}$ received encoded packets can be obtained according to (3) by taking the Kth entry of the $\tilde{M}$th iterated PMF $\boldsymbol{r}^{(\tilde{M})}$ as follows:

$$p_{\text{dec}}(K, \tilde{M}) = \mathbb{P}\left\{\text{rank } \tilde{\boldsymbol{G}}^{(\tilde{M})} = K\right\} = \boldsymbol{r}_K^{(\tilde{M})}. \tag{10}$$

The decoding performance is depicted in Fig. 2, which was created from 10^6 simulation runs. In Fig. 2a, the empirical PMFs of the required number of packets for successful decoding are shown. The figure also shows the analytical results for the random code, validating the derivation. It becomes evident that the random code requires less overhead than an LT code. This is because LT codes are optimized for efficient decoding when high values of K are present. For LT codes a random degree distribution is introduced to favor more sparse generator matrices, allowing an easier decoding. As usual, the robust soliton distribution is chosen for the degrees. However, using a degree distribution decreases the chances of i) increasing the rank of $\boldsymbol{G}$ by adding another column, i.e., (6) does not hold anymore, and ii) having an entry for each original packet at least once. As this work considers only a small number of packets that needs to be encoded, decoding complexity is not such a big concern, and we proceed with the random linear codes.

The figure also contains an LT code with an additional outer K-out-of-$\tilde{K}$ code that first encodes the original data into $\tilde{K} = K + 2$ precoded packets as a reference. Here, a reshaping of the PMF can be observed. By sacrificing good chances to have only zero or one additional packets required, the distribution tail is improved, leading to less likely worst-case scenarios. However, the completely random code outperforms both LT configurations.

Fig. 2b extends the results by studying different packet numbers K. Now, the complementary CDF (CCDF) is shown to focus on very high percentiles. Again, simulation results validate the derivation for random codes. All curves start at $\tilde{M} = K$, as this is the minimum required number for decoding in the best case. Again, the best performance can be observed

for the random code for the same reasons as described before. Furthermore, the outer code for LT improves the worst case scenario by making the curves steeper. However, the precoding also leads to a later decline.

In Fig. 3, the considered transmission schemes are illustrated, which will be explained subsequently in Sec. III and Sec. IV for single- and multi-user-scenarios, respectively.

III. THE SINGLE-USER CASE

First, we study our proposed MC schemes for single-user scenarios. We have conducted this analysis to a great extend already in [40]. However, our previous work contained a flaw, as explained in Section II-D, which is corrected here.

A. Transmission Schemes

1) Selection Combining (SC), cf. Fig. 3a: Here, copies of each of the K packets are sent simultaneously over each of the L available links. If at least one of these copies was transmitted correctly, the packet transmission was successful. Otherwise, a negative-acknowledgement (NACK) has to be fed back, containing information about which packet was affected such that a retransmission on all links can be initiated. As it can be seen in (1), each additional link with a reasonable individual PLR can dramatically improve reliability with respect to the overall PLR. However, this comes at a great cost, since each packet blocks several resources and there is no benefit if the transmission succeeds on more than one link, rendering it an inefficient scheme.

2) Rateless Coding (RC), cf. Fig. 3b: To address the potential resource wastage of SC, we propose to generate RC packets as long as necessary, which are distributed onto all available links. Thereby, each received packet contributes (with high probability) to the overall transmission. No NACKs are necessary, because the transmission can be pursued until one single acknowledgement (ACK) signalizes the success of the overall transmission. According to Fig. 2, already K (or only a few more) successfully transmitted packets are sufficient up to a very high probability.

The motivation is illustrated in Table IA. For illustration purposes, we consider two links with very high PLRs of 30% and 50%, respectively. Packet losses are depicted in red color. In the example, three of the ten original packets (2, 5, 6) are lost and have to be retransmitted (2', 5', 6'), when single-connectivity is implemented. One of the retransmissions (5') may fail, leading to 14 required transmissions on 14 radio resources in total.

When the second link is used as well, only one of the packets (6) is lost and the resulting retransmission (6') has better chances to be successful. Accordingly, this approach requires 11 times slots, but also 22 radio resources.

Finally, when RC is applied on the same two links, different encoded packets are sent, as indicated by the hat accent. In this realization, packet $\hat{17}$ is the 10th successful transmission. With a probability of around 30%, this best case is already sufficient. However, with a cumulative probability of almost 80% (95%), the transmission would be completed successfully, latest with the two successful transmissions of the 10th (11th) time slot.
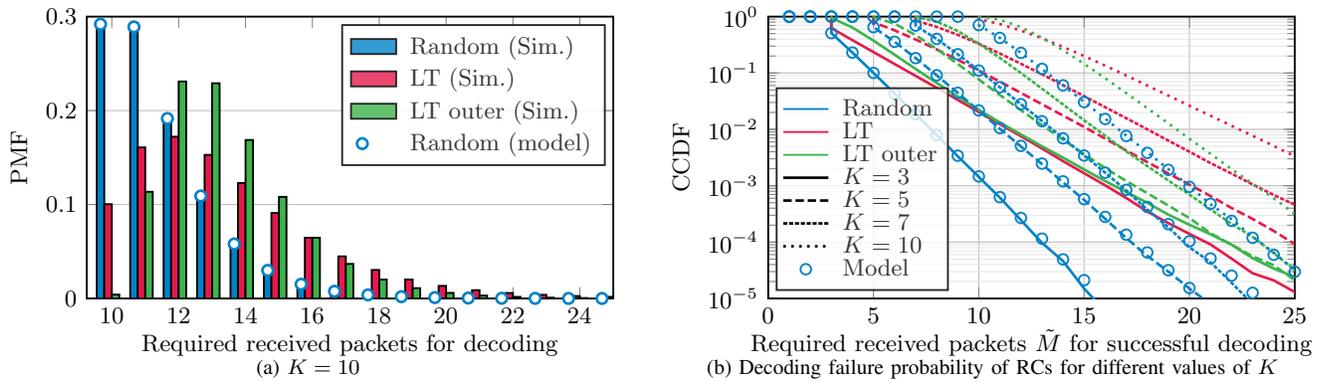
Fig. 2: Decoding performance obtained from simulation. For random linear fountain codes, analytical results are provided by markers. (a) Comparison of the required packets for successful decoding for random and LT codes. (b) Decoding probabilities for different K.
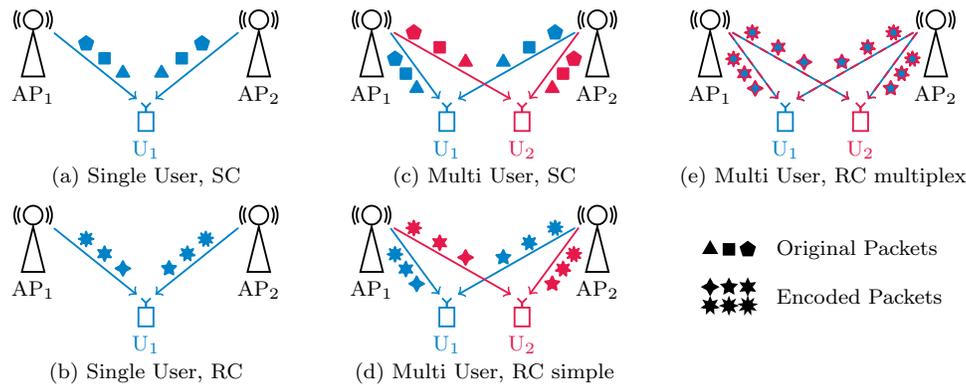

Fig. 3: Overview of considered transmission schemes for $L = 2$. In principle, the two sketched APs can also be co-located, exploiting frequency instead of spatial diversity. The single-user schemes (a),(b) are described in Sec. III, whereas multi-user schemes (c)-(e) are explained in Sec. IV.

TABLE I: ILLUSTRATION OF THE MC SCHEMES.

(A) SINGLE USER (SECTION III)

	Time Slot													
	1	2	3	4	5	6	7	8	9	10	11	12	13	14
SC ($L = 1$)														
Link 1	1	**2**	3	4	**5**	**6**	7	8	9	10	2′	**5′**	6′	5″
SC ($L = 2$)														
Link 1	1	**2**	3	4	**5**	**6**	7	8	9	10	6′	–	–	–
Link 2	1	2	**3**	**4**	5	6	7	8	**9**	10	6′	–	–	–
RC ($L = 2$) 30% 80% 95%														
Link 1	1̂	**3̂**	5̂	7̂	**9̂**	**1̂1**	1̂3	1̂5	1̂7	1̂9	2̂1	–	–	–
Link 2	**2̂**	4̂	**6̂**	8̂	1̂0	**1̂2**	1̂4	1̂6	**1̂8**	2̂0	2̂2	–	–	–

(B) MULTI USER MULTIPLEXING (SECTION IV-B)

		Radio Resource							
		1	2	3	4	5	6	7	8
SC ($L = 2$)	**User 1**	1	1	–	–	–	–	–	–
	User 2	–	–	2	2	–	–	–	–
	User 3	–	–	–	–	3	3	–	–
	User 4	–	–	–	–	–	–	4	4
RC ($L = 6$)	**User 1**	1̂	2̂	3̂	4̂	5̂	6̂	–	–
	User 2	1̂	2̂	3̂	4̂	5̂	6̂	–	–
	User 3	1̂	2̂	3̂	4̂	5̂	6̂	–	–
	User 4	1̂	2̂	3̂	4̂	5̂	6̂	–	–

Consequently, fewer resources have to be spent for the complete transmission than with SC of two links with high probability. However, in reality, links typically have lower PLRs than in the illustrative example, leading to a higher waste of resources for SC schemes, as it more likely that multiple links succeed without any benefit. The statistical advantages of RC will be analyzed in the subsequent sections.

B. Distribution of Required Radio Resources and Time Slots

To quantify the efficiency of the schemes at hand, the numbers of required radio resources R and occupied time slots T are analyzed in this section. For both KPIs, not only statistical moments (e. g., mean and variance) are of interest,

but the entire distributions in terms of their PMFs are derived. This is particularly important in the URC domain, because therein statements about very high percentiles (worst case scenarios) are required.

1) No Correlation in Time: First, we study the case that transmissions exhibit no correlation between consecutive time slots. This assumption ensures analytical tractability and holds for transmission time intervals (TTIs) that are longer than the channel's coherence time. Since the coherence time depends on the device speed and the carrier frequency, those factors together with the TTI determine whether the assumption is realistic for a given scenario. However, uncorrelated transmissions can also be achieved through techniques like channel

hopping [42]. In [43], a scheme is proposed that improves performance by switching channels only on bad conditions.

a) SC: The SC scheme is successful as soon as all original packets have been correctly received. Considering retransmissions of any missing packet, SC succeeds after K successful packet transmissions, which corresponds to a series of Bernoulli trials. Thus, for the earliest possible success after $M = K$ transmissions, all of them have to succeed. For a success after exactly $M > K$ transmissions, there must have been exactly $K - 1$ successful transmissions among the first $M - 1$ packets and the Mth transmission must have succeeded as well, because otherwise the transmission would have been completed earlier or later. With the success probability p_tx for each packet (cf. (1)) this leads to the following modified binomial distribution:

$$p_\text{rx}(K, M) = \begin{cases} 0, & M < K, \\ p_\text{tx}^K, & M = K, \\ \binom{M-1}{M-K} \bar{p}_\text{tx}^{M-K} p_\text{tx}^K, & M > K. \end{cases} \quad (11)$$

These probabilities already provide the PMF of the occupied time slots T for SC, since each transmission occupies one time slot. Hence, the PMF is given as follows:

$$f_T(t) = p_\text{rx}(K, t), \qquad t \in \mathbb{N}. \quad (12)$$

In each time slot, L links are used in parallel and, thus, the number of radio resources is given by $R = LT$. Accordingly, the respective PMF can be expressed as:

$$f_R(r) = \begin{cases} f_T\left(\frac{r}{L}\right), & \text{if } r = tL \text{ for } t \in \mathbb{N}, \\ 0, & \text{otherwise.} \end{cases} \quad (13)$$

b) RC: In the case of RC, each transmission conveys a distinct packet. We first consider the special case that all links are equally strong, i.e., $p_{\text{tx},l} = p_\text{tx}$ for $l \in \{1, \ldots, L\}$. Under this assumption, (11) can be used again to obtain the probability that K out of M transmissions are successful. However, it should be noted that now the probability p_tx of a single link is inserted, because now there are no duplications and each transmission has to be considered distinctive.

In the general case, the links exhibit different success probabilities $p_{\text{tx},l}$ for $l \in \{1, \ldots, L\}$, which corresponds to generalized Bernoulli trials. Now, the Mth packet is sent via the $(1 + M \bmod L)$th link and, thus, the Mth Bernoulli trial has a success probability $q_M = p_{\text{tx}, 1+M \bmod L}$.

Similarly to the iterative procedure in (8), the probability $\boldsymbol{p}_m^{(M)} = \begin{bmatrix} p_0^{(M)} & \cdots & p_M^{(M)} \end{bmatrix}$ of having m successful transmissions within M sent packets can be derived as follows:

$$\boldsymbol{p}^{(0)} = \begin{bmatrix} 1 & 0 & \cdots & 0 \end{bmatrix}, \quad (14)$$

$$\boldsymbol{p}_m^{(M+1)} = \begin{cases} \bar{q}_M \boldsymbol{p}_m^{(M)}, & m = 0, \\ \bar{q}_M \boldsymbol{p}_m^{(M)} + q_M \boldsymbol{p}_{m-1}^{(M)}, & m > 0. \end{cases} \quad (15)$$

Now, (15) provides the probability of successfully receiving exactly $\tilde{M}$ out of M packets as

$$p_\text{rx}(\tilde{M}, M) = \boldsymbol{p}_{\tilde{M}}^{(M)}. \quad (16)$$

The PMFs of the number of required resources R and time slots T can be derived from (16) for both cases, i.e., for

equally or unequally strong links. However, for RC the decoding success probability has to be incorporated as well. The scheme succeeds, if $\tilde{M}$ out of M packets are correctly received and sufficient for decoding. Thus, the cumulative distribution function (CDF) of the number of necessary sent packets S can be expressed as a sum of conditioned probabilities

$$F_S(M) = \sum_{m=K}^M \mathbb{P}\left\{ D(\tilde{M}) \mid \tilde{M} = m \right\}$$
$$= \sum_{m=K}^M p_\text{dec}(K, m) p_\text{rx}(m, M). \quad (17)$$

With (17), the success probability for exactly M sent packets, i.e., the PMF of S follows:

$$f_S(M) = p_\text{suc}(M) = \mathbb{P}\{S \leq M\} - \mathbb{P}\{S \leq M - 1\}$$
$$= F_S(M) - F_S(M - 1). \quad (18)$$

The derivation of the PMF of the number of required resources R has to take into account the fact that L links are used in each time slot simultaneously and, thus, only multiples of L radio resources are occupied. In other words, if a successfully transmitted packet on one link was sufficient to succeed, the transmissions via other links have been conducted anyways. Hence,

$$f_R(r) = \begin{cases} \sum_{l=0}^{L-1} p_\text{suc}(r - l), & \text{if } r \bmod L = 0, \\ 0, & \text{otherwise.} \end{cases} \quad (19)$$

Similarly, the PMF of occupied time slots T is obtained by summing the success probabilities of all numbers of packets that are reached by the considered scheme for each time slot t:

$$f_T(t) = \sum_{l=0}^{L-1} p_\text{suc}\left(\left\lceil \frac{t}{L} \right\rceil - l\right), \qquad t \in \mathbb{N}. \quad (20)$$

2) Channels with Time Correlation: The aforementioned derivations are not valid anymore if the transmissions are correlated, since in this case, subsequent transmissions are not independent Bernoulli trials anymore. However, this situation is barely tractable analytically and, hence, we provide simulation results for this case.

3) Feedback and Signaling Overhead: To compare the efficiency of the considered schemes, there are further relevant KPIs, namely the feedback that needs to be transmitted and possible signaling overhead for the coordination of the scheme.

a) Feedback: For SC, feedback is required at least for the failed packet transmissions, such that a retransmission can be initiated. Therefore, the NACK needs to contain an ID of the lost packet.[2] An even more reliable scheme would not only provide these NACKs, but also ACKs for each successfully transmitted packet, since the NACK feedback could also get lost and so a missing NACK does not ensure a successful transmission.

Since each NACK leads to a retransmission, the number N_NACK of necessary NACKs simply equals the number of

---

[2]Alternatively, the feedback process could be based on ACKs only, i.e., a retransmission would be initiated for each missing ACKs. However, for reasonable PLR< 0.5, NACKs are more efficient, since there are less failing than succeeding transmissions.

time slots exceeding the number of packets, i.e., $N_{\text{NACK}} = T - K$. If ACKs are involved as well, each package requires an ACK and so the number is $N_{\text{ACK}} = K$.[3]

It should be noted that each feedback (especially from the last packets) needs time and, thus, may introduce additional delay, which can span multiple time slots depending on the TTI length. However, the impact of this effect depends on the system and is not further investigated here.

For RC schemes, the feedback procedure is simple. Only one ACK signal in the end of a successful transmission is sufficient, because if packets are lost, no knowledge is required about which particular ones failed. The RC simply generates new packets as long as necessary. Thanks to the nature of RC no code rate has to be configured in advance.

By sending NACKs or ACKs as well, the knowledge could be exploited to avoid transmitting packets that correspond to columns of the generator matrix that do not provide further information with respect to the already received columns, thus increasing the decoding probability. However, developing such a strategy is out of scope in this work and left for further studies.

b) Signaling Overhead: In both schemes, only packet IDs have to be transmitted in addition to the payload. As already mentioned, by using the same PRNG on all involved devices the ID can be used to obtain the necessary column of the generator matrix for the RC scheme.

IV. THE MULTI-USER CASE

Now, we study the efficiency of RC-based schemes with U users. First, we simply apply the single-user schemes to all users, but afterwards, a more sophisticated scheme is studied.

A. Naive Extension of the Single-User Case

First, we assume that all users apply the SC and RC schemes from Section III, which is applicable in both UL and DL directions (cf. Fig. 3c,d). By considering multiple users, a statistical multiplexing gain will be achieved (cf. [44]). Since all users have a randomly varying need for resources (depending on their receiving conditions), not all of them need their peak amount of resources simultaneously. The total number R of necessary resources is the sum of the random variables R_u, containing the required numbers of resources of each user $u \in \{1, \ldots, U\}$. As all links are independent (Assumption 1), these numbers are independent and so the PMF of this sum results from convolution:

$$R = \sum_{u=1}^{U} R_u, \quad f_R = \mathop{\text{\LARGE $*$}}_{u=1}^{U} f_{R_u} := f_{R_1} * \ldots * f_{R_U}. \quad (21)$$

Other KPIs, such as the feedback, can be derived similarly as they also add up. However, the total number of time slots T requires rather a maximum than a sum operation, since all users can receive their data in parallel[4], and, thus, the overall duration depends on the last user. Hence, for independent links, the PMF of the number of required time slots can be expressed as follows:

$$T = \max T_u, \quad F_T(t) = \mathbb{P}\{\max T_u \leq t\} = \prod_{u=1}^{U} F_{T_u}(t). \quad (22)$$

B. Multiplexing with RC

Even though a higher efficiency can already be achieved through the statistical multiplexing gain (Section IV-A), a multi-user scenario provides an additional degree of freedom particularly in the DL. Now, there is more than one user and, thus, also more data. Therefore, we now consider that each user u wants to transmit K_u packets, such that there is a total of $K_{\text{all}} = \sum_u K_u$ packets to be transmitted. If all K_u are equal, this simplifies to $K_{\text{all}} = U K_u$.

1) Approach: Table IB illustrates the legacy SC scheme and our proposed transmission scheme for the multi-user DL[5] based on RC. In the conventional SC scheme, a fixed number of resources (here: $L = 2$) is assigned to each user, resulting in a total number of $L_{\text{all}} = L \cdot U$ required resources in each time slot. Each user receives the desired packet successfully as long as any of the L transmissions succeeds and, thus, the success rate is given by (1). Again, if more than one transmission is successful, their is no benefit and resources may be wasted. Transmission failures have to be communicated with a NACK feedback and packets have to be re-transmitted.

In contrast, we propose a code-multiplexing scheme for the DL, as sketched in Fig. 3e and in the lower part of Table IB. In total, L links are utilized, depending on how many resources are available and how many links the devices are capable to use in parallel. The data of all considered users is treated together, such that there are K_{all} packets of original data. The data is encoded with an RC code and broadcasted to all users on L links. It should be noted that in this scheme $L_{\text{all}} = L$. The example in Table IB motivates this approach. While SC with $L = 2$ uses eight links in total without retransmissions, our aim is that an RC multiplexing strategy utilizing only six links in total achieves the same success probability. We will derive these probabilities subsequently and provide a comparison of both approaches in Section VI.

A similar outcome could be achieved with a K-out-of-$\tilde{K}$ erasure code. However, this would require to fix the code rate a priori. RC provides the advantage that further packets can be added as necessary. The scheme can adjust to the number of available resources in a flexible manner and, instead of retransmissions, additional packets are generated and sent jointly to all users who have not been successful yet, even though different users might have lost different packets.

---

[3]This simple analysis does not incorporate the possibility that the feedbacks could get lost as well. However, this simple derivation provides a lower bound on the number and thereby already shows the advantages of RC over SC with respect to the feedbacks. Anyway, we can safely assume that signalling packets, like ACKs and NACKs, can be protected by strong coding and have a PLR orders of magnitude below that of data packets.

[4]Assuming that there is a sufficient number of channels available.

[5]As the proposed transmission scheme requires the knowledge of all data that has to be transmitted, it is only feasible for the DL. This approach does not induce any privacy issues, as the transmitted data has to be protected in wireless communications by other means, e. g., encryption, anyways.. The multi-user UL is not considered here and could be implemented using the single-user scheme from Section IV-A.

2) Distribution of Required Radio Resources and Time Slots: According to the scheme described above, a user receives encoded packets belonging to all users of the system, decodes all of them, if sufficiently many packets have been received, and picks the ones that are of interest for this specific user. In principle, it is sufficient to collect only packets until the users' packets can be decoded. However, we consider the condition that all original packets can be decoded, even though the data of other users is not of interest, because the analysis is much more tractable analytically. Hence, an upper performance bound is being derived.

Analogously to (17), the CDF of the number of required sent packets for a successful transmission, for a single user within this scheme can be derived by inserting $K = K_{\text{all}}$:

$$F_{S_u}(M) = \sum_{m=K_{\text{all}}}^{M} p_{\text{dec}}(K_{\text{all}}, m) p_{\text{rx}}(m, M). \quad (23)$$

For the entire system, the number of required packets is determined by the user who needs the most packets as the last ACK completes the transmission. Hence,

$$S = \max S_u, \quad F_S(s) = \mathbb{P}\{\max S_u \leq s\} = \prod_{u=1}^{U} F_{S_u}(s). \quad (24)$$

The PMFs of required radio resources and time slots of the entire system follow from (18)-(20).

C. Feedback and Signaling Overhead

For both described approaches in Sections IV-A and IV-B, the required feedback and signaling overhead behaves as in the single-user case (cf. Section III-B3). However, for SC, it cannot be obtained from the overall time slots, since the max operator hides the fact that some users might finish earlier. Therefore, the radio resources have to be considered: $N_{\text{NACK}} = \frac{R}{L} - K_{\text{all}}$. Optionally, $N_{\text{ACK}} = K_{\text{all}}$ ACKs might be transmitted. In contrast, for RC only one overall ACK per user is required, i.e., $N_{\text{ACK}} = U$ and no NACKs are necessary.

The signaling overhead is comparably low. In all schemes, users need to know on which channels they have to listen. However for RC, each user listens to more, but the same channels. Furthermore, the users need to know the total number K_{all} and the IDs of their own packets.

D. Computational Complexity

Especially for the multi-user multiplexing, the complexity at the user terminals should be discussed. This approach entails solving a linear system with K_{all} equations. With this, Gaussian elimination would be bounded by $\mathcal{O}(K_{\text{all}}^3)$ arithmetic operations. However, the matrix rows are only bits and, instead of floating point multiplications and additions, only xor operations are required, allowing a very efficient implementation that also does not suffer from numerical issues. By doing the element-wise xor in a row at once, e.g., through a 64-bit xor, the computational effort can be greatly reduced by this factor, such that the complexity rather appears quadratically for small K. Furthermore, by tracking the performed operations, new

columns due to additionally received packets, can be efficiently added to the decoding process without starting all over again.

V. SIMULATION SCENARIOS

In order to validate the derived models and to evaluate the performance of the considered schemes under time-correlated channels, numerical simulations were performed. For the sake of comparability, we evaluated the single-user scenario with the same parameters as in our previous work [40]. This way, we provide a correction to the flaw that was included therein. The scenario is recapped in Section V-A. However, for the multi-user scenario, we decided to extend the simulation settings by adding interference and using WiFi 6 as a realistic communications standard. The simulation parameters are specified in Section V-B.

With these two different configurations we also show a broader applicability for the proposed schemes. However, it should be noted that the feasibility rather depends on the (stochastic) characteristics of packet loss than on the technical details of the specific implementation, as the schemes are implemented on the application layer and thus technology-agnostic.

A. Simplified Communications Scenario

The scenario consists of three BSs located with an inter-site distance of $100\,\text{m}$, positioned at the vertices of an equilateral triangle. The BSs transmit with the constant power of $49\,\text{dBm}$. In order to obtain the average receive power P_{avg} from each BS at a given location, a standard 3GPP path loss model from [45] is used. A device uses the L strongest links, based on its measured average receive power P_{avg}, i.e., spatial diversity is used. The average receive power from the path loss model also serves as an input for simulating independent Rayleigh fading channels. The communications system is assumed to operate at the carrier frequency $f_{\text{c}} = 2.4\,\text{GHz}$. A device speed of $v = 10\,\text{m}\,\text{s}^{-1}$ is assumed, leading to an approximate coherence time of $T_{\text{coh}} \approx 5\,\text{ms}$ according to [46, (5.40.c)]. We differentiate between the time correlated and uncorrelated case by setting the sample time to $T_{\text{s,crr}} = 0.1\,\text{ms}$ and $T_{\text{s,uncrr}} = 10\,\text{ms}$, respectively. The classical Doppler spectrum is used, which relies on the assumption that various independent multi-path components arrive at the receiver solely in the horizontal plane, with equally distributed angle of arrivals and with no distinguishable time difference between the individual multipath components.

In this proof-of-concept scenario, a simple criterion is used to determine whether a packet is received correctly or not. Whenever the instantaneous receive power $P(t)$ at a time instant t is larger than a given threshold $P_{\text{min}} = -55\,\text{dBm}$, i.e.,

$$P(t) \geq P_{\text{min}} \quad (25)$$

the packet transmission starting at time t is considered successful and lost otherwise. A more sophisticated approach is described in Section V-B, where a WLAN setup is simulated.

TABLE II: WiFi 6 Simulation Parameters.

Parameter	Value
Channel model	
Fading	flat Rayleigh fading
Doppler	classical
Carrier frequency	5.2 GHz
Relative velocity	$\{1\,\mathrm{m\,s^{-1}}, 30\,\mathrm{m\,s^{-1}}\}$
PHY-transmitter	
Modulation and coding	MCS0 (BPSK, code rate 0.5)
System bandwidth	20 MHz
Resource unit size	26 subcarriers
PPDU size	30 Byte
Guard interval	0.8 μs
Channel coding	binary convolutional coding
Transmit antennas	1
PHY-receiver	
Receiving antennas	1
Carrier frequency offset	none
Timing synchronization	realistic
Frequency synchronization	pilot phase tracking
Channel estimation mode	2xHE-LTF

Based on the criterion (25) and the Rayleigh distribution, the PLR of each link l can be expressed as

$$\bar{p}_{\mathrm{tx},l} = 1 - \exp\left(-\frac{1}{P_{\mathrm{avg},l} - P_{\min}}\right). \tag{26}$$

In order to elaborate on the impact of differently strong links we consider two configurations:

(A) A device is located at the center of the three BSs, leading to an equal PLR $\bar{p}_{\mathrm{tx},l} = 0.11$ on each link ($l \in \{1, 2, 3\}$).

(B) A device is located at a fixed location $17\,\mathrm{m}$ away from the center. With this, the PLRs with respect to the three BSs are $\bar{p}_{\mathrm{tx},1} = 0.04$, $\bar{p}_{\mathrm{tx},2} = 0.11$, and $\bar{p}_{\mathrm{tx},3} = 0.24$.

To obtain statistics, $N_{\mathrm{U}} = 10^6$ channel realizations are simulated. In each, $K = 10$ packets have to be transmitted and retransmissions are performed until the transmission is successful. The choice $K = 10$ turned out to already offer benefits in the single user case as will be shown in Sec. VI-A. The impact of the packet number will be discussed in more detail in Sec. VI-D.

B. WLAN Scenario

In order to assess the multi-user scenario, *MathWorks' WLAN toolbox* from *MATLAB r2018b* was utilized to produce more realistic packet error sequences. Not only fast fading, but also the interference from other WLAN transmissions was taken into account as a cause of failure. Therefore, the evaluation does not rely on a simplified condition like (25) but rather on the simulation of a practical system.

For this assessment, the parameters for generating the channel were altered compared to Section V-A to reflect a realistic WLAN scenario. Devices are placed at a position in the area between three APs at the corners of an equilateral triangle, which are separated by an inter-site distance of $50\,\mathrm{m}$ from each other. The position is moved from the center to the location at the distances of 17, 35, and $39\,\mathrm{m}$ to the three APs, respectively, such that there is a strong serving AP and two weaker interfering APs. We do not further vary the positions and signal strengths here, as this would involve many

additional degrees of freedom. A more general analysis is left for further studies.

To investigate correlated and uncorrelated channels in time, two different velocities of the devices are considered, i. e., $v_{\mathrm{crr}} = 1\,\mathrm{m\,s^{-1}}$ and $v_{\mathrm{uncrr}} = 30\,\mathrm{m\,s^{-1}}$, respectively. With this configuration, a PLR of approximately $\bar{p}_{\mathrm{tx},1} = 0.11$ is achieved for the serving AP in the uncorrelated case. This value is plugged into the analytical equations for their evaluation.

WiFi 6 packets are generated and transmitted over the simulated channel realizations. WiFi 6, also known as IEEE 802.11ax, is the successor of IEEE 802.11ac and IEEE 802.11n, which are widely spread and can be found in almost every consumer device today. We have chosen WiFi as a communications standard for evaluation, due to its extreme dissemination. Consumer communications standards, like WiFi, already find application in certain industrial scenarios [47]. URLLC applications in particular could benefit from the novelties introduced in WiFi 6 as analyzed in [48]. One of the major novelties is the addition of orthogonal frequency division multiple access (OFDMA), which was now incorporated in WiFi for the first time. With OFDMA more users can be served in parallel and more finely granulated resources can be provided.

The PHY configuration for this scenario was chosen to allow for a reliable operation and is briefly explained here. Packets are generated with the smallest possible system bandwidth of $20\,\mathrm{MHz}$. The available bandwidth is divided among the maximum number of users for this bandwidth $U = 9$, therefore, each user is getting 26 subcarriers for payload transmission assigned. The smallest available modulation and coding scheme (MCS) utilizing binary phase-shift keying (BPSK) modulation and code rate 0.5 is chosen, which allows for the most robust transmission. For channel coding, the available convolutional code was preferred and the smallest available guard interval of $0.8\,\mathrm{μs}$ was used to generate the packets. To keep the scenario simple we are not using MIMO and instead are transmitting and receiving with a single antenna. The receiver implements realistic time- and frequency synchronization. Furthermore, frequency synchronization is improved by using the pilots in the data portion of the packet. A reduced channel estimation mode is used, where channel estimation is only carried out for every second subcarrier and interpolated in between. This achieves good results in channels with low frequency selectivity as used here, while reducing the overhead of the preamble.

The generated packets of the serving AP are interfered by WiFi 6 packets from two neighboring APs. The packets of the interfering APs are generated with the same parameters as for the serving AP. To prevent that synchronization fields of the interfering APs add up constructively to the desired transmission and hence improve decoding probability, the packets of the interfering APs are randomly delayed in time domain for each sent packet. It is assumed that both interfering APs transmit one packet after another without any break between the transmission.

The link realizations of $N_{\mathrm{U}} = 10^5$ users have been simulated for each setting to obtain the statistics. However, since multiple users are served simultaneously, the number of

realizations for the statistics is only $N_{\mathrm{sim}} = \frac{N_{\mathrm{U}}}{U}$. The main simulation parameters are summarized in Table II.

VI. Numerical Validation and Evaluation

Based on the simulation scenarios from Section V, this section provides a numerical validation of the derived models and a comparison of the considered schemes with respect to their efficiency.

A. Single User

At first the considered schemes will be studied in a single-user scenario. Thereby, we revise our previous work in [40]. The results are depicted in Fig. 4. The figure shows the CCDFs of required radio resources R and required time slots T for a successful transmission of $K = 10$ packets in the upper and lower part, respectively. On the left hand side, i. e., subplots (a) and (b), channels without correlation in time are considered. In contrast, the remaining subplots on the right were generated for correlated channels in time. Accordingly, only the axes on the left contain markers that indicate analytical model results as our mathematical framework is only applicable in the uncorrelated case. As a last differentiation, the experiments were conducted for the single user scenarios (A) and (B), i. e., equally strong (a,c) and differently strong links (b,d).

1) Uncorrelated Channels in Time: First, it can be observed that all analytical results, which are indicated by markers, match the empirical CCDFs from simulations very well. It also becomes evident that analytical values are available for much lower probabilities, since simulations become infeasible for extremely low outage rates (each additional order of magnitude in the CCDF increases the computation time by approximately 10). For the same reason, the simulation results are less reliable for the tail values of the empirical CCDF.

As for the radio resources, from the upper subplots in (a) and (b) it can be observed that the curves of the RC schemes start much earlier to decline than their SC counterparts for $L \in \{2, 3\}$. This is reasonable, because the MC schemes based on SC require at least $K \cdot L$ radio resources for a successful transmission. Depending on the receiving conditions and the decoding probability, the RC schemes require much less radio resources in most of the cases. For equally strong links, both RC curves meet the SC curve of $L = 2$ at a CCDF value of approximately 10^{-3}, meaning that less resources are required in around $99.9\,\%$ of the cases. In this regard, SC with $L = 3$ performs even worse. Thus, even though the curves are less steep for RC than for SC, their advantage up to very high percentiles renders RC a much more efficient scheme[6]. This finding is confirmed by comparing the mean values, which are indicated by filled markers. It can further be noted that

[6] It should be noted that the CCDF plots should not be confused with reliability plots. The focus here lies rather on the resource efficiency, as reliable transmissions can be ensured with fewer resources in the majority of the cases, which is an important issue with respect to the system capacity with multiple URC users or users from other services who can benefit from the saved resources. The low CCDF values only become an issue if there is also a latency constraint. As it will be shown in the subsequent sections, the RC schemes outperform SC also at lower CCDF values when multiple users are present.

for equally strong links, the curves of the RC schemes only differ in the step size, since without correlation, it does not matter on how many links data is distributed. For unequally strong links, SC and RC show a similar behavior as before for $L = 2$. However, RC with $L = 3$ suffers from the bad performance of the weak third link.

So far, the single-link scheme (SC, $L = 1$) was not considered. In terms of radio resources it outperforms all other schemes as expected, as it only transmits exactly what is needed through retransmissions. However, the figure does not reflect the fact that each retransmission requires a NACK on the feedback channel. Therefore, additional radio resources are required for SC, which are not included in the CCDF of radio resources. Thereby, it should be noted that even though the feedback messages carry less payload than data packets, they have to be transmitted very reliably, and failures in the feedback have an additional negative impact, which was not studied here. Furthermore, the entire transmission may take a very long time, also leading to a longer allocation of feedback resources. This is shown in the lower part of the figure, where the distributions of time slots are depicted. Here, single connectivity exhibits the worst performance.

Regarding the time slots, the schemes with $L = 3$ finish earlier than $L = 2$, as they use more frequency diversity and, thus, require less diversity in time. By definition, the SC schemes require at least $T = K$ time slots for the entire transmission. Again the slopes, which become more steep with each link, are less steep for the RC schemes. However, they can benefit from their head start. If latency is an issue, the number of links could be increased even more, such that available data is distributed in the frequency or spatial domain, leading to an earlier and steeper decrease of the RC curves. Furthermore, the time slots are an indicator for the number of required NACKs for the SC schemes by looking on the time slots exceeding $K = 10$. Here, a benefit of the RC schemes becomes evident, as they always require only one ACK.

2) Correlated Channels in Time: As the modeling was only carried out without time correlation, no model results are available in this case. Now, the behavior changes a little. Regarding the radio resources, the RC schemes outperform their SC counter parts in approximately $90\,\%$ of the cases and in the mean. In the higher percentiles there is a region, where SC shows better performance, after which both schemes share approximately the same tail. It should be noted that, due to the log scale, the major $90\,\%$ part takes only a small part of the figure.

Due to the time correlation, all schemes exhibit very long tails, as devices may become stuck in deep fades, which lead to many consecutive packet losses. By adding more links, it is not possible to avoid them completely, but the probability can be lowered by an order of magnitude, as long as the links are strong enough. As it can be seen in Fig. 4d (top), the performance of $L = 3$ suffers from utilizing the weakest third link by wasting resources there. Utilizing more links also leads to a steeper decrease of the tails for the time slot distributions. Here, the RC schemes provide an efficient way to add more links to benefit from these diversity gains.
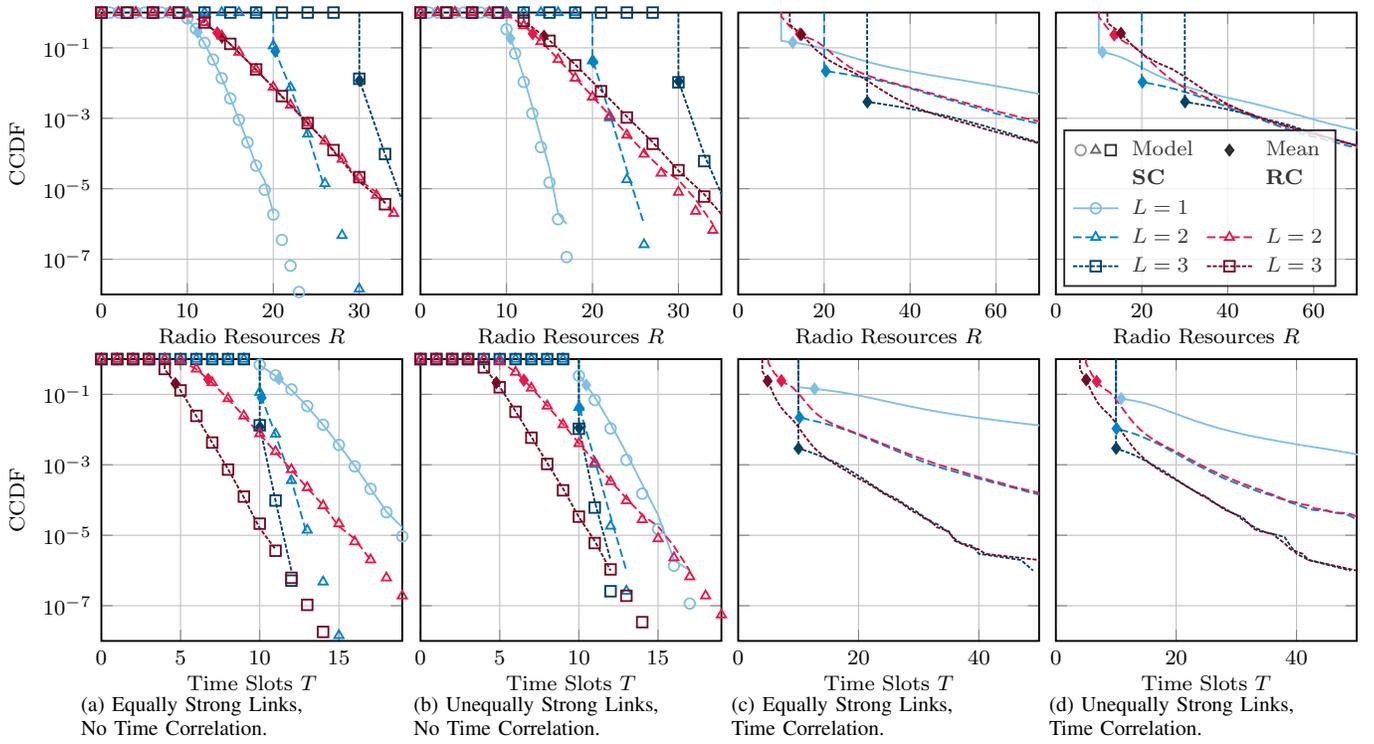
Fig. 4: Distributions of required radio resources R and time slots T. Results are shown for equally (odd) and unequally strong links (even), respectively. Furthermore, the experiments are conducted with (right) and without time correlation (left). The legend applies to all plots. Markers indicate model results and mean values whereas lines refer to simulations. The figure revises the results of our previous work [40].
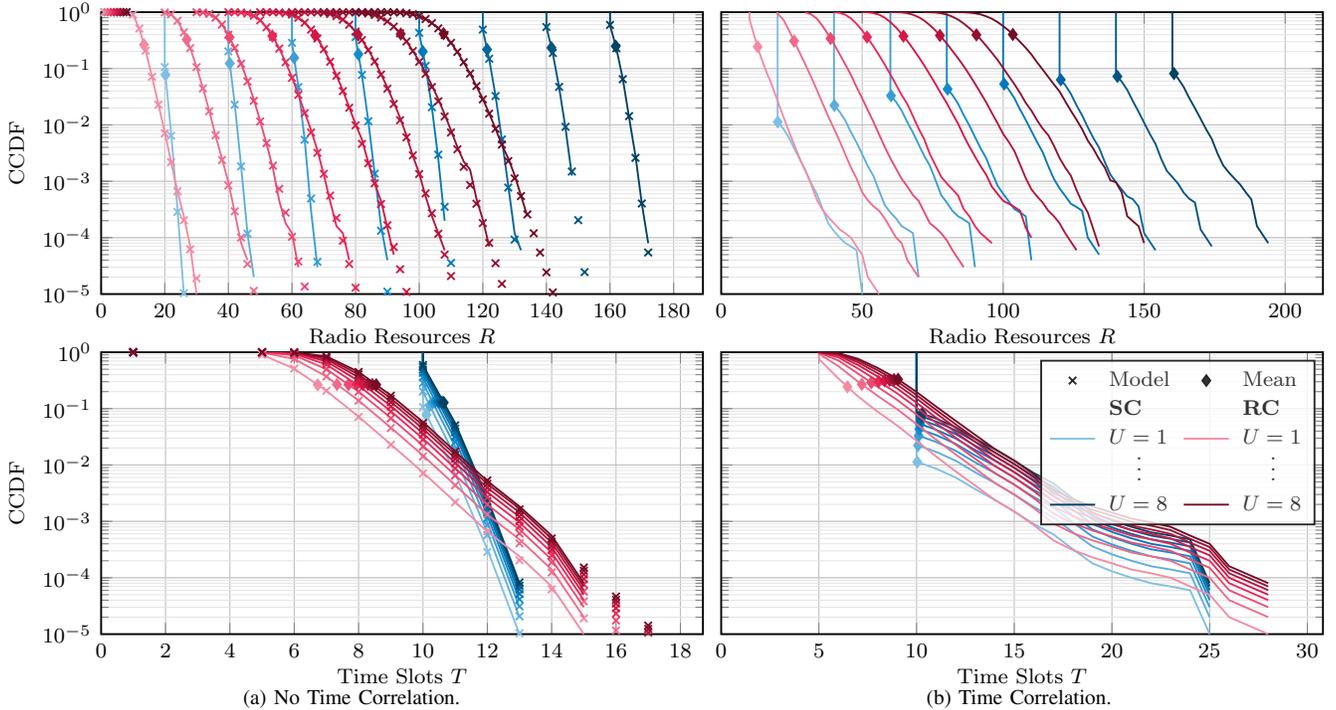

Fig. 5: Evaluation of the multi-user approach that simply extends the single user case for $K = 10$ packets and $L = 2$ links per user.

B. Single-User Scheme in a Multi-User Scenario

As now the number of users is introduced as another degree of freedom, we restrict the parameter space by only considering equally strong links and focusing on the schemes with $L = 2$, as they have shown the best performance in the single user case. The results are depicted in Fig. 5 for the required radio resources (top) and time slots (down), as well as in the cases with uncorrelated (left) and correlated (right) channels in time.

First, it can be noted that again the model (markers) and the simulation results (lines) match very well in the uncorrelated case. Also, the model can go far lower with respect to extremely low probabilities (as desired for URC) and the empirical CCDFs become inaccurate at the tail.

Second, when looking at the radio resources, the behavior is similar to the single-user case. However, the gaps between both schemes increase with the number of users, leading to much later intersections of the curves (up to almost impossible probabilities), which was expected, as the curves result from a convolution of the single-user case (cf. (21)). This effect is also called *statistical multiplexing*, i.e., the total number of required radio resources (which is related to the system capacity) is not just the single-user performance times the number of users. In particular, the distribution tail performance is much better than this product, since it is very unlikely that *all* users experience the worst case scenario. To see this, one can exemplary compare the RC curves in Fig. 5a (top) at the probability 10^{-4}. Whereas one user requires 30 or less resources in $1 - 10^{-4}$ of the cases, eight users require 140, which is only a factor of less than five instead of eight. For the correlated case (Fig. 5b top) the factor at the same values is only three.

Third, the time slot behavior is also similar to the single-user case. However, now the single-user results are combined by a maximum operation (cf. (22)). Thereby, only the worst of the users is considered, leading to curves that are very close to each other, especially for higher number of users. Accordingly, the RC schemes perform better up to a high percentile. Only in the correlated case, there is an area (approximately 50% to 90%), where the RC schemes take slightly longer for a higher number of users.

Lastly, it should be noted that the total number of NACKs for SC cannot be read directly from the time slots plots anymore, as they are showing only the maximum number of feedbacks of all users. However, the total number of NACKs is included in the radio resources, as it is the number of radio resources exceeding the total packet number ($K_{\mathrm{all}} = K \cdot U$) divided by the number of links. Thus, the radio resources plots of SC are only a shifted and scaled version of the feedbacks. Hence, as the gain in radio resource usage increases with the number of users, it likewise improves for the feedback efficiency.

C. Multi-User Multiplexing Scheme

The power of multiplexing gains could be already observed in the previous section, where it just came from considering multiple users together statistically. Now, we study our approach where we multiplex the data of multiple users together. As this increases the total amount of data, we can decrease the data per user that is involved to $K = 5$.

We also change the number of links to $L = 6$ for the RC scheme, while keeping two links for SC per user. This might seem unfair at the first glance, but in the RC scheme all users share the same resources (even though they have different receiving conditions), such that the RC always uses six links in total, no matter how many users are in the system. In contrast,

the total number of links increases for SC. However, applying the total number of links from the respective SC scheme, might render unrealistic for higher numbers of users, since RC users would have to be able to listen to many links (unnecessarily).

The results are depicted in Fig. 6 with the same discrimination into subplots as in Fig. 5. As with the previous studies, the model is confirmed by the simulation results and the model can go to much lower probabilities whereas the simulation results show inaccuracies at the tail.

Compared with Fig. 5 all x-axes are scaled down, which is mostly due to the fact that we decreased the payload K of each user. However, for the RC schemes more significant gains with respect to the radio resources can be observed for a higher number of users.

In the time-correlated case (Fig. 6b top), the RC schemes now exhibit steeper slopes than their SC counter parts. This is due the fact that now all users can benefit from a higher diversity in frequency, as they can all use $L = 6$ links. Consequently, higher diversity gains can be observed even though less links may be utilized in total (for more than three users).

As for the time slots, the situation now differs for RC, since here the payload now increases with each additional user and so it is not just the maximum of the single user performance anymore. Accordingly, a few more time slots are required in both the time-correlated (Fig. 6b) and uncorrelated (Fig. 6a) case for five or more users as a price for the more efficient scheme. This comes also from the fact that only $L = 6$ links are used in total, such that the overall payload has to be distributed more over time. Hence, if the time is important, this behavior can be easily improved by spending more links to all devices, as long as this is technically feasible, which would also further improve the slopes in the correlated case.[7] Compared to the SC scheme, which uses 16 links in total for eight users, there is still some potential.

In this regard, it should also be noted that devices which are not capable in listening to so many links, could be easily included into this scheme without further ado. Since the RC scheme is flexible by definition, such a device could just use some of the links, which of course comes with performance degradation, but does not require any additional management.

Considering the feedback, the RC scheme with multiplexing renders the same efficiency as discussed in Section IV-A. Each user only has to send an ACK as soon as the relevant data can be decoded, whereas the SC schemes require NACKs for each failed packet transmission.

D. Impact of Parameters K, L and PLR

Lastly, the impact of varying parameters on the multiplexing scheme is discussed. Therefore, mean values are plotted in Fig. 7 to reduce the number of curves, even though this approach hides the tail behavior. In general, correlation in time has only little impact on the mean values, as it mainly affects tails behavior, i.e., values with extremely low probabilities.

---

[7]The radio resources would not be affected by changing the number of links in the uncorrelated case except for the step size, because again it does not matter on how many links the data is distributed.
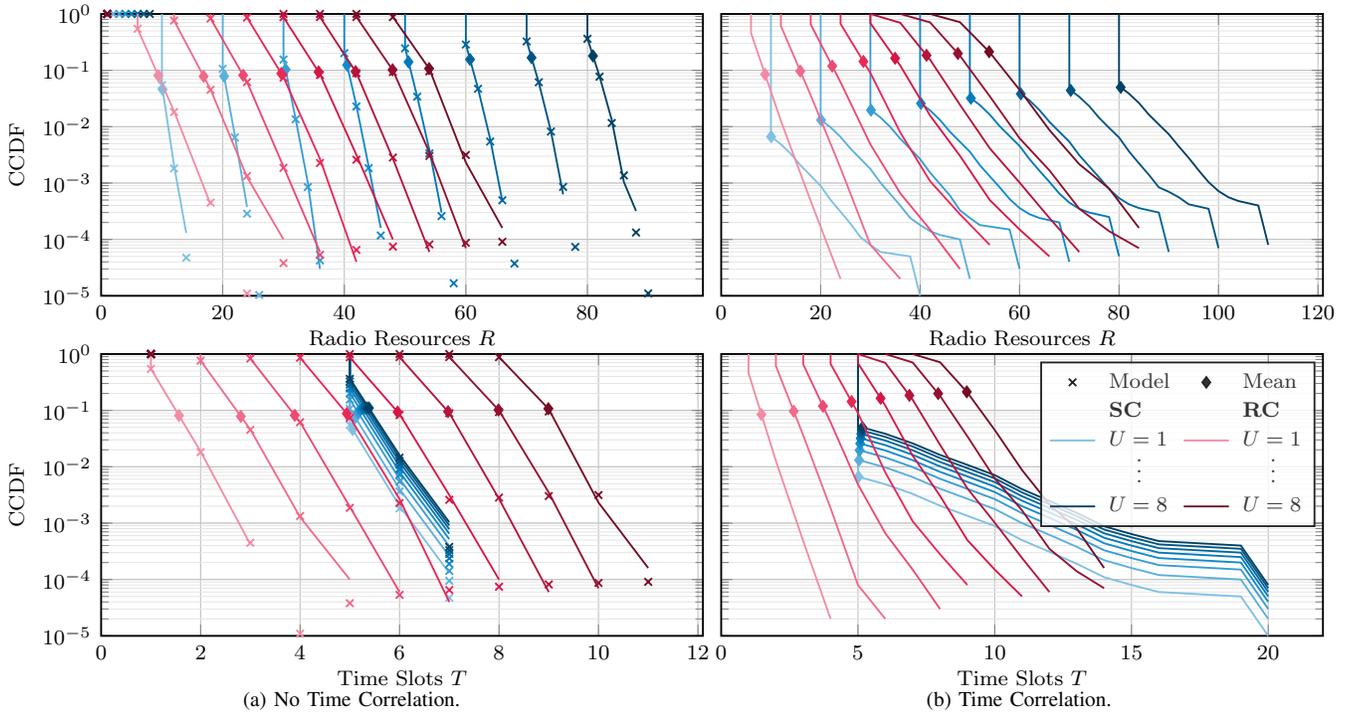
Fig. 6: Performance evaluation of the multi-user multiplexing approach for $K = 5$ packets per user. The SC scheme provides $L = 2$ links per user, whereas for RC all users share a fixed number $L = 6$ of links, i.e., the data is broadcasted.
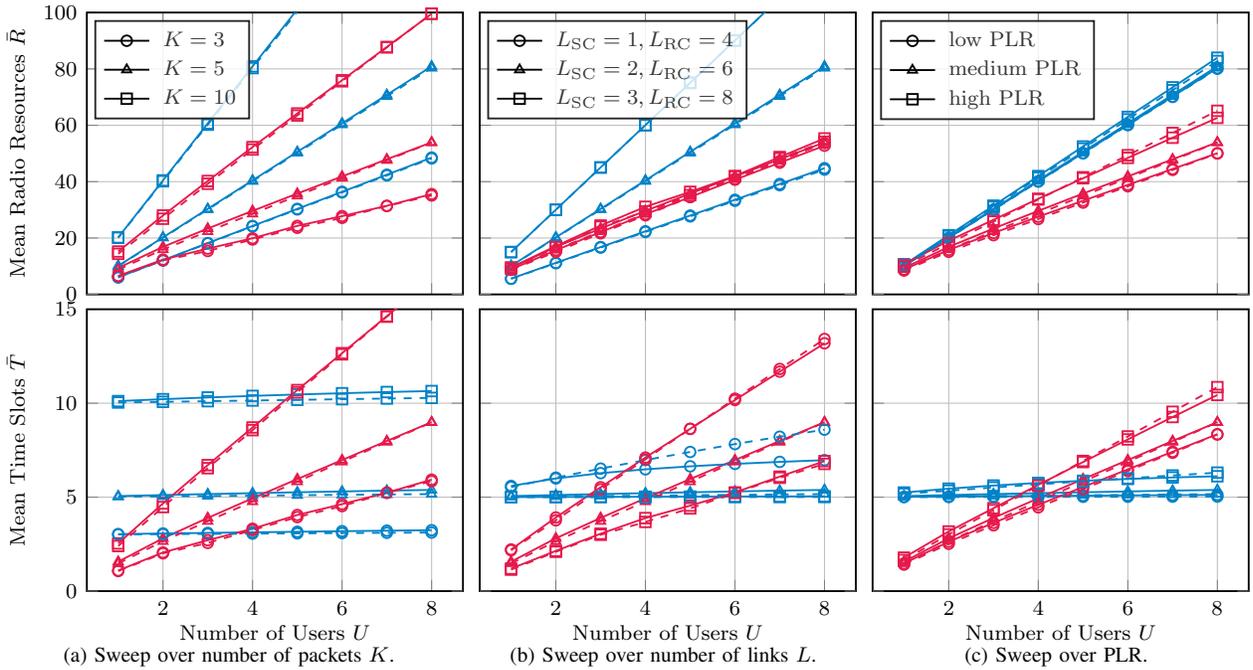

Fig. 7: Impact of different parameters on the mean performance of SC (blue) and RC with multiplexing (red). Solid and dashed lines refer to uncorrelated and correlated channels, respectively. The value in the middle always denotes the default.

Therefore, solid lines (no correlation) and their dashed counterparts (with correlation) almost coincide.

Fig. 7a clearly shows an increasing gain on resource efficiency of RC over SC with increasing packet number K or number of users U. In particular, for a low number of users U, a certain packet number is required to be able to observe an outperformance of RC over SC. For instance $K = 3$ (5)

packets require at least three (two) users to be more efficient with respect to the mean and is equal otherwise. However, this gain has to be traded off with the number of time slots (cf. lower part).

The number of links L clearly increases the resource usage of SC (cf. Fig.7b), but has almost no impact for RC, as resources are just distributed more in frequency than in time.

Consequently, the link number is a good means to reduce the number of required time slots. Furthermore, a higher L improves the tail performance (not visible in the mean plot). This way, the RC scheme offers much more diversity to all users at a relatively low cost in terms of radio resources. Thereby, the scheme enables a simple way to always utilize all available radio resources.

For different PLRs (Fig. 7c) the device was moved, leading to $\bar{p}_{tx} \in \{0.22, 0.11, 0.06\}$ on each link in the uncorrelated case. For SC the impact on the mean is small, since with to links the chances of losing a packet are small for all considered PLRs. However, for RC the gains over SC increase with lower PLR, as it benefits more from the single link PLR.

VII. CONCLUSION AND OUTLOOK

In the light of ultra-reliable communications (URC), adding diversity through multi-connectivity (MC) is one if not the best enabler. However, redundancy usually implies wasting resources in conditions where it turns out that it was not necessary, leading to inefficient use of radio resources. In order to recapture efficiency, we have proposed strategies to apply rateless codes (RCs) to URC, which by their nature adapt the code rate to the conditions at hand. Our analysis comprises both, single- and multi-user scenarios, and our proposed schemes have shown significant benefits, when compared to selection combining (SC).

In particular, the RC schemes are more efficient, as they require fewer resources in the majority of cases and in the mean. As for the required feedback, they always outperform SC. The achievable gains can be further improved, when more than one user is considered. Thereby, the total capacity of the system is increased.

In general, the benefits of the proposed RC schemes are increased under a higher payload, either by combining more packets of one user or by adding users to the code. Furthermore, our multiplexing scheme requires fewer packets per user, making it more attractive for low-latency applications. For time-correlated channels, the multiplexing scheme has the additional benefit of all users enjoying greater frequency diversity.

Our multi-user multiplexing approach is primarily limited by the maximum number of parallel links that devices are able to utilize. However, our approach can be applied at the application level and does not require strict coordination among links. This facilitates combining different radio interfaces to obtain more parallel links. Furthermore, devices that support only few parallel links can easily be integrated into the scheme. Also, additional links (e. g., from other base stations (BSs)) can be easily added, for instance, to prepare handovers.

Our models can help engineers tailor wireless systems to their requirements, available resources, and expected channel conditions (e. g., with respect to packet loss and correlation) more efficiently. Depending on the application, they may find a suitable trade off between time and frequency diversity.

These benefits can be achieved at the comparably low cost increased decoding complexity and little to no signaling overhead. We expect the complexity increases to be very manageable. However, if complexity becomes an issue, raptor codes may be a good alternative to random linear fountain codes, as raptor codes feature linear encoding and decoding as well as excellent decoding probabilities. The use of raptor codes in this manner is left to future work.

Further studies may investigate more realistic scenarios, e. g., including mobility, correlation in space and frequency, and maybe use sophisticated system-level simulators or real-world radio testbeds. We also see potential in studying the feedback process and optimizing the generator matrix based on acknowledgements (ACKs) at a packet-level for the RC schemes.

ACKNOWLEDGMENT

REFERENCES

[1] ITU-R, "IMT vision – framework and overall objectives of the future development of IMT for 2020 and beyond," International Telecommunication Union - Radiocommunication Sector, Rec. ITU-R M.2083-0, 9 2015.

[2] P. Popovski et al., "Wireless access in ultra-reliable low-latency communication (URLLC)," IEEE Trans. Commun., vol. 67, no. 8, pp. 5783–5801, 2019.

[3] M. Bennis, M. Debbah, and H. V. Poor, "Ultrareliable and low-latency wireless communication: Tail, risk, and scale," Proc. IEEE, vol. 106, no. 10, pp. 1834–1853, 10 2018.

[4] P. Popovski, "Ultra-reliable communication in 5G wireless systems," 1st Int. Conf. 5G Ubiquitous Connectivity, pp. 146–151, 2014.

[5] 5GPPP, "Automotive vision," 5GPPP, White Paper, 8 2015.

[6] L. Scheuvens et al., "Framework for adaptive controller design over wireless delay-prone communication channels," IEEE Access, vol. 7, 4 2019.

[7] 3GPP, "Technical specification group services and system aspects; service requirements for the 5G system; stage 1 (release 16)," Tech. Spec. TS 22.261 V16.12.0, 2020.

[8] A. Pradhan and S. Das, "Joint preference metric for efficient resource allocation in co-existence of eMBB and URLLC," in Int. Conf. Commun. Syst. Netw. (COMSNETS), 2020, pp. 897–899.

[9] Z. Li et al., "5G URLLC: Design challenges and system concepts," in ISWCS, 2018, pp. 1–6.

[10] K. S. Kim et al., "Ultrareliable and low-latency communication techniques for tactile Internet services," Proc. IEEE, vol. 107, no. 2, pp. 376–393, 2019.

[11] S. Lien et al., "Efficient ultra-reliable and low latency communications and massive machine-type communications in 5G new radio," in IEEE GLOBECOM, 2017, pp. 1–7.

[12] B. Chang et al., "Optimizing resource allocation in URLLC for real-time wireless control systems," IEEE Trans. Veh. Technol., vol. 68, no. 9, pp. 8916–8927, 2019.

[13] L. Scheuvens et al., "Wireless control communications co-design via application-adaptive resource management," in 2nd IEEE 5G World Forum (5GWF), 2019, pp. 298–303.

[14] J. Sachs et al., "5G radio network design for ultra-reliable low-latency communication," IEEE Netw., vol. 32, no. 2, pp. 24–31, 2018.

[15] M. Simsek et al., "On the Flexibility and Autonomy of 5G Wireless Networks," IEEE Access, vol. 5, 2017.

[16] J. J. Nielsen, R. Liu, and P. Popovski, "Ultra-reliable low latency communication using interface diversity," IEEE Trans. Commun., vol. 66, no. 3, pp. 1322–1334, 3 2018.

[17] A. Wolf et al., "How reliable and capable is multi-connectivity?" IEEE Trans. Commun., vol. 67, no. 2, 2019.

[18] 3GPP, "Technical specification group radio access network; evolved universal terrestrial radio access (E-UTRA); study on small cell enhancements for E-UTRA and E-UTRAN – higher layer aspects (rel. 12)," TR 36.842 V1.0.0, 11 2013.

[19] E. Dahlman, S. Parkvall, and J. Sköld, "Chapter 20 - final thoughts," in 4G LTE/LTE-Advanced for Mobile Broadband. Oxford: Academic Press, 2011, pp. 411 – 415.

[20] B. U. Kazi and G. A. Wainer, "Next generation wireless cellular networks: ultra-dense multi-tier and multi-cell cooperation perspective," *Wirel. Netw.*, vol. 25, no. 4, pp. 2041–2064, 5 2019.

[21] G. Mountaser, T. Mahmoodi, and O. Simeone, "Reliable and low-latency fronthaul for tactile Internet applications," *IEEE J. Sel. Areas Commun.*, vol. 36, no. 11, pp. 2455–2463, 11 2018.

[22] D. J. C. MacKay, "Fountain codes," *IEE P-Commun.*, vol. 152, no. 6, pp. 1062–1068, 12 2005.

[23] M. Luby, "LT codes," in *43rd Annu. IEEE Symp. Found. Comput. Sci. Proc.*, 2002, pp. 271–280.

[24] A. Shokrollahi, M. Luby *et al.*, "Raptor codes," *Found. Trends Commun. Inf. Theory*, vol. 6, no. 3–4, pp. 213–322, 2011.

[25] M. Luby *et al.*, "RaptorQ Forward Error Correction Scheme for Object Delivery," Internet Requests for Comments, RFC Editor, RFC 6330, 8 2011.

[26] M. Zhang, C. Li, and S. Kim, "Efficient utilization of rateless LDPC codes for satellite broadcasting services," in *8th Int. Conf. Wirel. Commun. Signal Process. (WCSP)*, 2016, pp. 1–5.

[27] C. Anglano, R. Gaeta, and M. Grangetto, "Exploiting rateless codes in cloud storage systems," *IEEE Trans. Parallel Distrib. Syst.*, vol. 26, no. 5, pp. 1313–1322, 2015.

[28] S. Kim and S. Lee, "Rateless erasure resilient codes for content storage and distribution in P2P networks," in *11th Int. Conf. Adv. Commun. Technol.*, vol. 01, 2009, pp. 444–446.

[29] 3GPP, "Technical specification group services and system aspects; multimedia broadcast/multicast service (MBMS); protocols and codecs (release 15)," Tech. Spec. TS 26.346 V15.5.0, 2020.

[30] S. Tian *et al.*, "A physical-layer rateless code for wireless channels," *IEEE Trans. Commun.*, vol. 61, no. 6, pp. 2117–2127, 2013.

[31] M. Shirvanimoghaddam, Y. Li, and B. Vucetic, "Multiple access analog fountain codes," in *IEEE ISIT*, 2014, pp. 2167–2171.

[32] M. Shirvanimoghaddam *et al.*, "Probabilistic rateless multiple access for machine-to-machine communication," *IEEE Trans. Wireless Commun.*, vol. 14, no. 12, pp. 6815–6826, 2015.

[33] Y. Zhang *et al.*, "Rateless coded multi-user downlink transmission in cloud radio access network," *Mobile Networks and Applications*, Dec 2018.

[34] ——, "Rateless coded uplink transmission design for multi-user C-RAN," *Sensors*, vol. 19, no. 13, p. 2978, Jul 2019.

[35] J. Castura and Y. Mao, "Rateless coding for wireless relay channels," *IEEE Trans. Wireless Commun.*, vol. 6, no. 5, pp. 1638–1642, 2007.

[36] Yijia Fan *et al.*, "Rateless coding for MIMO block fading channels," 2008, pp. 2252–2256.

[37] M. M. Shanechi, U. Erez, and G. W. Wornell, "Rateless codes for MIMO channels," in *IEEE GLOBECOM*, 2008, pp. 1–5.

[38] M. M. Shanechi *et al.*, "Time-invariant rateless codes for MIMO channels," in *IEEE ISIT*, 2008, pp. 2247–2251.

[39] J. Bao and H. Li, "Multi-connectivity using erasure code for reliable transmission in millimeter wave communications," in *IEEE Int. Conf. Commun. (ICC)*, 2019, pp. 1–6.

[40] P. Schulz, A. N. Barreto, and G. Fettweis, "Efficient and reliable wireless communications through multi-connectivity and rateless coding," in *IEEE Wirel. Commun. Netw. Conf. (WCNC)*, 4 2020, pp. 1–6.

[41] T. Ho *et al.*, "The benefits of coding over routing in a randomized setting," in *IEEE ISIT*, 2003.

[42] A. A. M. Saleh *et al.*, "An experimental TDMA indoor radio communications system using slow frequency hopping and coding," *IEEE Trans. Commun.*, vol. 39, no. 1, pp. 152–162, 1 1991.

[43] T. Hößler *et al.*, "Dynamic connectivity for robust applications in Rayleigh-fading channels," *IEEE Commun. Lett.*, vol. 24, no. 2, pp. 456–460, 2020.

[44] J. Chaudhary, J. Bartelt, and G. Fettweis, "Statistical multiplexing and pilot optimization in fronthaul-constrained massive MIMO," *EURASIP J. Wirel. Comm.*, vol. 2018, no. 1, Aug 2018.

[45] 3GPP, "Technical specification group radio access network; evolved universal terrestrial radio access (E-UTRA) - Further advancements for E-UTRA: Physical layer aspects," Tech. Rep. TR 36.814 V9.0.0, 2010.

[46] T. S. Rappaport, *Wireless communications principles and practice*. Upper Saddle River, NJ: Prentice Hall, 1996.

[47] A. Frotzscher *et al.*, "Requirements and current solutions of wireless communication in industrial automation," in *IEEE Int. Conf. Commun. Workshops (ICC)*, 2014, pp. 67–72.

[48] A. Traßl *et al.*, "On dependability metrics for wireless industrial communications - applied to IEEE 802.11ax," in *2nd IEEE 5G World Forum (5GWF)*, 2019, pp. 286–291.

Philipp Schulz (Member, IEEE) received the M.Sc. degree in mathematics and the Ph.D. (Dr.-Ing.) in electrical engineering from Technische Universtität Dresden (TU Dresden), Germany, in 2014 and 2020, respectively. He was a research assistant at TU Dresden in the field of numerical mathematics, modeling, and simulation. In 2015, he joined the Vodafone Chair Mobile Communications Systems at TU Dresden and became a member of the system-level group. His research there focused on flow-level modeling and the application of queuing theory on communications systems with respect to ultra-reliable low latency communications. After more than one year at the Barkhausen Institut, Dresden, Germany, where he investigated rateless codes in the context of multi-connectivity, he is now back at the Vodafone Chair and studies spectrum sensing and localization.

Andreas Trassl Andreas Traßl received the Dipl.-Ing. degree in electrical engineering from Technische Universität Dresden in 2018. Currently, he is pursuing the Ph.D. degree in wireless communications in Dresden. He investigates methods to realize the tight requirements of ultra-reliable low-latency communications in a resource-efficient manner. His research interests also include the WLAN physical layer and wireless industrial communications.

André Noll Barreto (Senior Member, IEEE) received the M.Sc. degree in Electrical Engineering from Catholic University (PUC-Rio), Rio de Janeiro, Brazil, in 1996, and the Ph.D. degree in Electrical Engineering from Technische Universität Dresden, Germany, in 2001. He held several positions with academia and industry in Switzerland (IBM Research) and Brazil (Claro, Nokia Technology Institute/INDT, Universidade de Brasília, and Ektrum) before joining the Barkhausen Institut, Dresden, Germany, in 2018. He was the Chair of the Centro-Norte Brasil Section of the IEEE in 2013 and 2014, and the General Co-Chair of the Brazilian Telecommunications Symposium in 2012.

Gerhard Fettweis (Fellow, IEEE) received the Ph.D. degree under supervision of Prof. H. Meyr's from RWTH Aachen in 1990. He has been the Vodafone Chair Professor with TU Dresden since 1994 and the Head of the Barkhausen Institute since 2018. After one year with IBM Research, San Jose, CA, USA, he moved to TCSI Inc., Berkeley, CA, USA. He coordinates the 5G Lab Germany, and has coordinated two German Science Foundation (DFG) centers at TU Dresden, namely cfaed and HAEC. In Dresden, his team has spun-out seventeen start-ups, and setup funded projects in volume of close to EUR 1/2 billion. In 2019, he was elected into the DFG Senate. His research focuses on wireless transmission and chip design for wireless/IoT platforms, with 20 companies from Asia/Europe/U.S. sponsoring his research. He also serves on the board of National Instruments Corp, and advises other companies. He is a Co-Chair of the IEEE 5G/Future Networks Initiative, and has helped organizing IEEE conferences, most notably as a TPC Chair of ICC 2009 and TTM 2012, and as a General Chair of VTC Spring 2013 and DATE 2014. He is a member of the German Academy of Sciences (Leopoldina), the German Academy of Engineering (acatech), and received multiple IEEE recognitions as well has the VDE ring of honor.